The Astrophysical Journal, 727:42 (5pp), 2011 January 20 doi:10.1088/0004-637X/727/1/42

A STUDY OF A NEW INCREASING SUBMILLIMETER SPECTRAL COMPONENT OF AN X28 SOLAR FLARE

A. H. Zhou[1], J. P. Li[1], and X. D. Wang[2]
[1] Purple Mountain Observatory, Chinese Academy of Sciences, Nanjing 210008, China
[2] Hohai University, Nanjing 210098, China
Received 2010 March 12; accepted 2010 November 10; published 2010 December 30

ABSTRACT

In this paper, we study a novel spectral component that increases with frequency above 200 GHz in an X28 solar flare that occurred on 2003 November 4. A maximum flux density of ∼20,000 sfu was observed at 405 GHz at main phase. We model its spectra based on gyrosynchrotron (GS) radiation computations in the case of a magnetic dipole field. Our computations show that the new increasing submillimeter spectral component at the main peak P1 can be generated by energetic electrons with a harder spectral index (2.3), low-energy cutoff of 30 keV, and number density of 10^{10} cm^{-3} in a compact source (0.″5 radius) with a strong local magnetic field varying from 780 to 4590 G via GS emission. The associated microwave (MW) spectral component can be produced by energetic electrons via GS emission, but with a 10 keV low-energy cutoff and number density 1.2×10^6 cm^{-3} in an extended source (40″ radius) with mean magnetic field strengths from 100 to 576 G. The MW and submillimeter emission sources, inferred from the magnetic dipole field model, are located in the corona and ∼1000 km low atmosphere levels above the photosphere, respectively. Energy flux, energy loss rate, and total energy released by energetic electrons are estimated for the first time. It is found that the energy flux can attain values of 7.2×10^{13} erg cm^{-2} s^{-1} in the submillimeter source. This value is four orders higher than that in the MW source. The energies released by electrons in the submillimeter and MW sources reach, respectively, 1.2×10^{32} and 1.9×10^{31} erg. The total energy released by energetic electrons is 1.4×10^{32} erg during the flare in the MW and submillimeter sources. The mean energy released by energetic electrons for a subsecond pulse, i.e., the fragment energy, is estimated to be about 5.2×10^{26} erg.

Key words: Sun: flares – Sun: radio radiation

1. INTRODUCTION

Solar flares are a consequence of magnetic instabilities in the solar atmosphere. Within seconds to minutes, a large amount of magnetic energy is released into the acceleration of charged particles, a shock wave, and heat. A broad spectrum of electromagnetic radiation is emitted, from km wavelengths to γ-rays. The energy production processes in solar flares can be investigated from their emission spectra at various wavelength ranges. It is well known that the main radiation mechanism at microwave (MW) wavelengths is generally thought to be gyrosynchrotron (GS) radiation from $\geqslant$10 keV electrons. However, solar flare emission at frequencies above 100 GHz (THz band) is poorly known. To extend the frequency range of flare observation above 100 GHz, a Solar Submillimeter Telescope (SST) was built (Kaufmann et al. 2001). Since the first detection of solar flares (Trottet et al. 2002) in the submillimeter band above 200 GHz, more than 10 additional flares have been observed in this band (Silva et al. 2007). These flare observations revealed a new phenomenon: when simultaneous data at lower radio frequencies are also available, two different types of spectral behavior are obtained. For some of these flares, the emission observed at 212 GHz is consistent with extrapolation of the lower frequency GS emission from MW to submillimeter wavelengths (Trottet et al. 2002; Kaufmann et al. 2002; Raulin et al. 2004; Lüthi et al. 2004). In contrast, Kaufmann et al. (2004) found a new increasing spectral component that increases with frequency above 200 GHz in the 2003 November 4 solar flare. The source of this new increasing submillimeter spectral component is uncertain.

Possible explanations for the new spectral component so far include thermal free–free emission from an optically thick source (Ohki & Hudson 1975), synchrotron emission from relativistic electrons (Stein & Ney 1963) or positrons (Murphy et al. 1987; Trottet et al. 2004; Trottet 2006), emission of plasma waves excited by relativistic electron beams (Sakai et al. 2006) or by proton beams (Sakai & Nagasugi 2007), incoherent synchrotron radiation by a microbunching instability (Kaufmann & Raulin 2006), diffusive radiation, and Cherenkov emission (Fleishman & Kontar 2010). Recently, Silva et al. (2007) presented evidence that GS emission of the increasing submillimeter spectral component occurred in the 2003 November 2 flare under a uniform magnetic field assumption, but in which an extreme value of the magnetic field (4500 G) and a high electron number density of 1.7×10^{12} cm^{-3} are required. These requirements can be decreased by using the GS radiation calculation in a nonuniform magnetic field model (Zhou et al. 2010). In this paper, we will study the increasing submillimeter spectral component of the solar burst that occurred on 2003 November 4.

Another purpose of this paper is to try to evaluate the energy released by energetic electrons during solar bursts. In general, radio burst spectroscopy should have the potential to diagnose the energetic electrons and magnetic fields in radio sources, but either additional assumptions or data are usually necessary to separate the properties of the electron distribution from the magnetic fields. Several papers (e.g., Batchelor et al. 1984; Dulk 1985; Gary 1985; Bastian & Gary 1992; Lim et al. 1992) tried to estimate the magnetic field on the basis of the simplified relations of the GS radiation (Dulk & Marsh 1982), all using several additional assumptions. To decrease the number of these assumptions a more direct method was presented by Zhou & Karlicky (1994), using Dulk & Marsh's simplified relations. The diagnostic formula of magnetic fields was improved further (Zhou et al. 1998; Zhou & Wang 2000) with more accurate simplified relations for the GS radiation in the longitudinal and transverse propagation cases. Once the magnetic field strength can be estimated, the electron information can also be obtained.

We note that in the above studies a homogeneous source assumption was usually adopted. This work provides a different approach, i.e., by fitting the observational spectrum via GS computations of an inhomogeneous source and thus obtaining information about the energetic electrons and magnetic fields involved.

In this paper, we will study in detail the increasing submillimeter and MW spectral components of the 2003 November 4 flare. For this event the possibility of a new spectral component produced by microbunching instability has been discussed, but with the requirement of very high energy electrons (Kaufmann & Raulin 2006). In this paper, we will further study the possibility of GS radiation of the submillimeter and MW spectral components produced by the 2003 November 4 flare and model the spectra based on the GS radiation calculations in a magnetic dipole field case. In the GS emission calculation, we consider an energetic electron distribution that is isotropic in pitch angle and power law in energy. Here we emphasize that the self-absorption and gyroresonance should be considered simultaneously in the absorption calculation, especially for emission at the low frequencies of the MW spectrum in the strong magnetic field and lower density ($N < 10^5$ cm^{-3}) regions of nonthermal electrons (Zhou et al. 2004). We try to determine whether the GS radiation may be responsible for the new increasing submillimeter spectral component and what the conditions needed to produce this new component are. The flare observations are described in Section 2. Section 3 shows the spectral fits of the increasing submillimeter and MW emissions. Energy flux, energy loss rate, and total energy released by energetic electrons are estimated in the submillimeter and MW sources for the first time in Section 4. Section 5 presents the discussion and conclusions.

2. OBSERVATIONS

The hard X-ray emission from the very large ("giant") solar flare on 2003 November 4 was observed by the hard X-ray/gamma-ray spectrometer on the *Ulysses* spacecraft. The early rise part of the giant flare and part of the decay of the hard X-ray emission associated with the giant flare were also observed by the hard X-ray imager on the *RHESSI* satellite. The maximum of the hard X-ray emission during the giant flare could not be observed by the *RHESSI* instrument because of satellite night. The Hα flare (importance 3B) was located at S19, W83 in the active region (AR) NOAA 10486. *GOES* observations of the associated soft X-ray emission show that the soft X-ray maximum occurred at ~1947 UT with peak flux of *GOES* class $\geqslant$X28 (Kane et al. 2005).

Ulysses observed an increase in 25–150 keV X-rays from 1933 to 2015 UT with the maximum at ~1944 UT, almost simultaneously with the maximum in 15.6 GHz radio emission and ~3 minutes before the maximum in the soft X-ray emission. This indicates that the X-ray emission observed by *Ulysses* was mostly nonthermal. The total energy in >20 keV electrons released during the flare is estimated to be $\sim 1.3 \times 10^{34}$ erg. Ovens Valley Solar Array (OVSA) radio observations show that the flare produced intense MW emission, the peak flux at 15.6 GHz being ~42,000 sfu at ~1945 UT. It is interesting that the SST detected a remarkable new burst spectral component that increases with frequency above 200 GHz. The new emission component has three major peaks in time and originated in a compact source (Kaufmann et al. 2004). Intense subsecond pulses superposed on the bulk emission also increase with frequency. The maximum flux density of the bulk emission

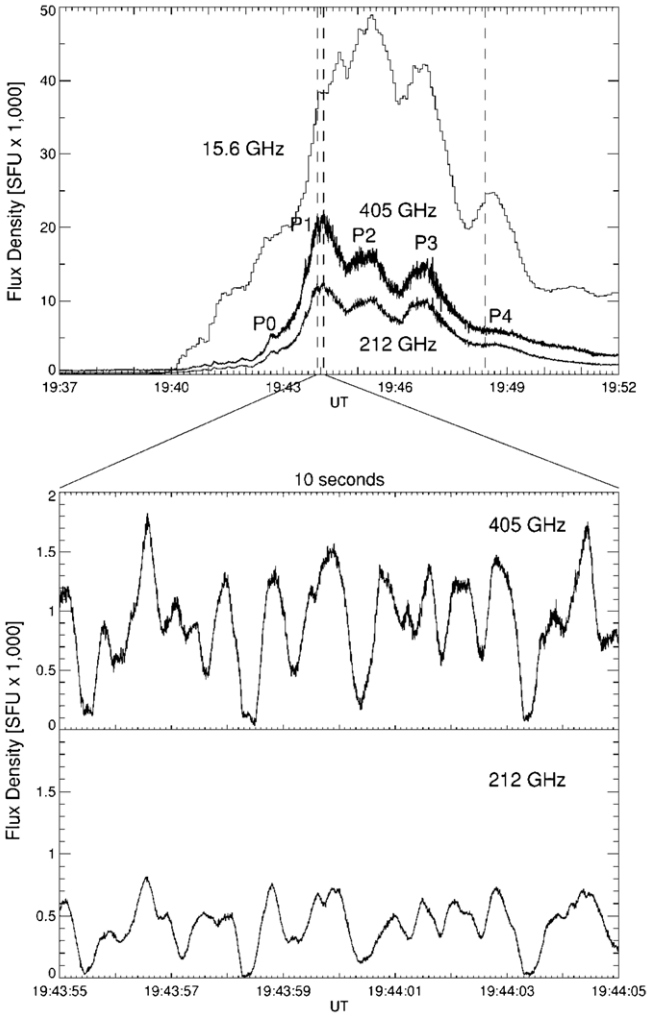

Figure 1. Time profiles of the burst at 405, 212, and 15.6 GHz (top) obtained, respectively, with SST and OVSA in units of thousands of solar flux units. An example of the intense subsecond pulses is shown over a 10 s period during the first peak P1 at the bottom (Kaufmann et al. 2004).

reaches as high as ~20,000 sfu at 405 GHz, which is two times higher than that at 212 GHz. The time profiles at 212 and 405 GHz are shown at the top of Figure 1. This flare displays similar shapes for the time profiles from 15.6 GHz through 405 GHz to the hard X- and γ-rays, which implies that these emissions are produced by the same accelerated electrons during this flare. The observations with high time resolution exhibit fine structure at those frequencies. Figure 1 (bottom) shows an example of the intense submillimeter pulses over a 10 s period during peak P1, with 5 ms time resolution, showing the superposed rapid pulses with the main bulk emission subtracted.

The radio spectra from MW to submillimeter emissions exhibit two distinct components (see Figure 2), the new component with increasing intensities for higher frequencies into the terahertz range, i.e., the broadband 0.1–100 THz (1 THz = 10^{12} Hz), and the MW component with intensities decaying for higher frequencies. OVSA 1.2–18 GHz MW data are shown in Figure 2 for the major peak P1 and minor peak P4 for which 44 GHz data were obtained by Itapetinga Radio Observatory (Kaufmann et al. 2004). A sample of the mean spectrum for the pulse flux in excess of the bulk emission is also shown in Figure 2 for structure P1.

Table 1
The Burst Source Parameters for the Submillimeter (THz) and MW Components

Peak	B_0(G)	θ°	R''	h_d(cm)	h_u(cm)	B_u(G)	B_d(G)	$\bar{B}$(G)
P1 (THz)	5000	80	0.5	1×10^8	3×10^9	780	4590	2690
P4, P1(THz pulse)	5000	80	0.25	1×10^8	3×10^9	780	4590	2690
P1 and P4 (MW)	2000	80	40	1.8×10^9	6×10^9	100	576	338

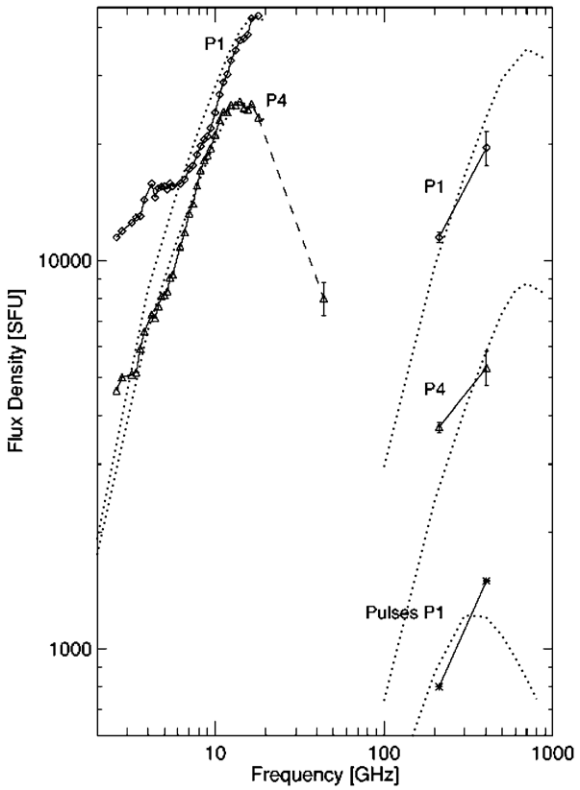

Figure 2. Calculated GS emission spectra (dotted lines) superimposed on the submillimeter data from SST, MW data from OVSA at peaks P1 and P4, and the mean spectrum of the flux of pulse emission at peak P1 from SST (see the original Figure 4 given by Kaufmann et al. 2004).

3. FITS FOR THE MW AND INCREASING SUBMILLIMETER SPECTRAL COMPONENTS

In this paper, we model the radio burst spectra based on the GS radiation calculations in the case of a magnetic dipole field (Zhou et al. 2004). A set of burst source parameters was selected to fit the submillimeter and MW spectral components of the 2003 November 4 burst (see Table 1): B_0 and R are the photosphere magnetic field strength and source radius (in arcsec), respectively, and h_d and h_u are the heights of the lower and upper boundaries of the burst source, respectively. B_d, B_u, and $\bar{B}$ (G) are, respectively, the magnetic field strengths at the lower and upper boundaries, and their mean value. The energy spectral index of energetic electrons, δ, can be obtained from a more accurate expression (Zhou et al. 1998),

$$\delta = (\alpha + 0.59)/0.79, \quad (1)$$

where α is the observational spectral index in the optically thin part, which can be estimated from the flux densities at the peak frequency and 44 GHz of the MW range (α = 2.3 for peak P4). We assume that α is constant over peaks P1–P4 during the main phase. We used the flare longitude $\sim 80^\circ$ as the viewing angle. We set the high-energy cutoff at

Table 2
The Physical Parameters of Energetic Electrons

Peak	δ	E_0(keV)	E_m(MeV)	N(cm^{-3})
P1 (THz)	2.3	30	10	10^{10}
P4 (THz)	2.3	30	10	5.5×10^9
P1 (THz pulse)	2.3	30	10	8.5×10^7
P1 (MW)	2.3	10	5	1.2×10^6
P4 (MW)	2.3	10	5	6×10^5

$E_m = 10$ MeV for the submillimeter emission. It was found that the low-energy cutoff E_0 can substantially affect the spectral calculations (Zhou et al. 2008) and the estimate for total energy released by energetic electrons in the submillimeter burst region, so we selected a sequence of values of E_0 from 20 to 100 keV for the submillimeter emission. We find that the best value for the submillimeter spectral fit at peak P1 is for $E_0 = 30$ keV. The lower boundary height of the burst source, h_d, can also substantially affect the spectral calculation, so h_d was set as low as possible (200–1000 km above the photosphere) to avoid this influence. It is found that a value for h_d of 1000 km is enough for accurate spectral calculations for the lower frequencies of the THz band. It is shown that the modeled GS spectrum in the submillimeter frequency range (see the dotted line in Figure 2) can fit the observational results at the main peak P1 in the magnetic dipole field case for $E_0 = 30$ keV, $N = 10^{10}$ cm^{-3}, and $B_0 = 5000$ G, i.e., local magnetic field strength of 780–4590 G range (with a mean value of 2690 G; see Table 1). The intense MW spectrum at peak P1 can be fitted by the GS radiation; however the low-energy cutoff E_0 must be carefully selected. Because it strongly influences the fit at lower frequencies in the optically thick part and also the estimate for total energy released by energetic electrons in the MW burst region, a sequence of E_0 from 10 to 50 keV was selected for the fit of the observed MW spectrum. It was found that the best fit, shown in Figure 2, for the MW component of peak P1 occurs for $E_0 = 10$ keV, $N = 1.2 \times 10^6$ cm^{-3}, and $B_0 = 2000$ G, i.e., local magnetic field strength of 100–576 G range (with a mean magnetic field of 338 G). For the peak P4 of the submillimeter emission, the required low-energy cutoff is 30 keV and the number density is 5.5×10^9 cm^{-3}, i.e., about one-half of the number density of the main peak P1. On the other hand, the number density (6×10^5 cm^{-3}) of the MW source for peak P4 also decreased to half its value as compared with that for peak P1 (see Table 2).

The flux densities of intense subsecond pulses superposed on the bulk emission also increase with frequency. The pulse emission spectrum at peak P1 can also be fitted by the GS radiation for a low-energy cutoff of 30 keV and electron number density of 8.5×10^7 cm^{-3} and the fit for the pulse emission spectrum is good (see Table 2).

4. THE ENERGY FLUX CARRIED BY THE ENERGETIC ELECTRONS

Once the number density N is obtained from the numerical fit to the observed spectrum, the distribution function of energetic

Table 3
The Energy Flux and Total Energy Carried by the Energetic Electrons in the 2003 November 4 Burst

Peak	$N(\mathrm{cm}^{-3})$	N_{total}	G	$E_F(\mathrm{erg\,cm^{-2}\,s^{-1}})$	$E'(\mathrm{erg\,s^{-1}})$	$E(\mathrm{erg})$
P1 (THz)	10^{10}	1.0×10^{34}	1.1×10^{12}	7.2×10^{13}	3.0×10^{29}	1.2×10^{32}
P4 (THz)	5.5×10^{9}	1.8×10^{33}	6.0×10^{11}	3.9×10^{13}	4.0×10^{28}	...
P1 (THz pulse)	8.5×10^{7}	2.8×10^{31}	9.2×10^{9}	6.0×10^{11}	6.2×10^{26}	...
P1 (MW)	1.2×10^{6}	1.0×10^{34}	3.1×10^{7}	1.8×10^{9}	4.8×10^{28}	1.9×10^{31}
P4 (MW)	6.0×10^{5}	5.0×10^{33}	1.6×10^{7}	9.4×10^{8}	2.5×10^{28}	...

electrons $n(E)$ can be determined. The energy flux carried by energetic electrons can also be estimated by

$$E_F = \int_{E_0}^{E_m} E v n(E) dE \,(\mathrm{erg\,cm^{-2}\,s^{-1}}), \quad (2)$$

where v is the velocity of energetic electrons. Substituting $n(E) = GE^{-\delta}$ into the above equation, we get

$$E_F = \frac{3G}{2.5-\delta}\left(E_m^{2.5-\delta} - E_0^{2.5-\delta}\right) (\delta \neq 2.5),$$

$$E_F = 3G \ln(E_m/E_0) \,(\delta = 2.5), \quad (3)$$

where E_0 and E_m (keV) can also be obtained from the numerical fit to the observed spectrum. Substituting the physical parameters obtained from the spectral fit into the above expression, the energy flux carried by energetic electrons can be estimated. Then the energy loss rate E' (erg $\mathrm{s^{-1}}$) and the total energy E (erg) carried by energetic electrons in the submillimeter and MW sources can also be calculated (see Table 3), where the source radii were, respectively, 0.″5 and 40″ for the submillimeter and MW sources for the main peak P1, with a 400 s lifetime (the full width at half-maximum for the burst time profile; see Figure 1).

It is shown in Table 3 that the energy flux E_F carried by the energetic electrons can reach 7.2×10^{13} (erg $\mathrm{cm^{-2}\ s^{-1}}$) in the submillimeter source for the main peak P1, but in the MW source it only reaches 1.8×10^{9} (erg $\mathrm{cm^{-2}\ s^{-1}}$), which is four orders of magnitude lower than that of the submillimeter source. For the main peak P1, the energy loss rate E' reaches 4.8×10^{28} erg $\mathrm{s^{-1}}$ in the MW source and 3.0×10^{29} erg in the submillimeter source, which is about five times higher than that of the MW source due to the strong submillimeter emission loss. The energies E released by electrons in the submillimeter and MW sources reach, respectively, 1.2×10^{32} and 1.9×10^{31} erg, i.e., a total energy of 1.4×10^{32} erg in the two sources during the flare. The total energy 1.4×10^{32} erg obtained from the submillimeter and MW observations is about two orders of magnitude lower than 1.3×10^{34} erg estimated from the hard X-ray emission (Kane et al. 2005) and two times higher than the value of about 5×10^{31} erg estimated from the *GOES* observation for the emission measure (EM) and temperature (T). The electron number densities in the submillimeter source are much higher than those in the MW source for the peaks P1 and P4 (see Table 3), but the total numbers of energetic electrons in the MW source can attain 1.0×10^{34} and 5.0×10^{33}, which are close to the values in the submillimeter source, due to a larger MW source size.

The energy flux and energy loss rate for the pulse emission are, respectively, 6.0×10^{11} erg $\mathrm{cm^{-2}\ s^{-1}}$ and 6.2×10^{26} erg $\mathrm{s^{-1}}$. Figure 1 shows that there are about 12 subsecond pulses within the 10 s time sample, so the mean energy released by energetic electrons for a pulse is estimated to be 5.2×10^{26} erg.

5. DISCUSSION AND CONCLUSIONS

Several emission mechanisms have been proposed so far to account for the new increasing submillimeter spectral component. Although thermal free–free emission always exists, such sources would produce too much flux in ultraviolet and soft X-ray wavelengths (Kaufmann & Raulin 2006; Silva et al. 2007). Therefore, the submillimeter emission component is more properly associated with nonthermal mechanisms. The possibility of THz synchrotron emission by positrons has been discussed for another event. However, the required number of positrons to produce the observed THz flux is considerably larger than what is inferred from X-ray and γ-ray observations (Kaufmann & Raulin 2006; Silva et al. 2007). The THz emission from Langmuir waves excited by relativistic electron beams precipitating into the high-density solar photosphere has been simulated (Sakai et al. 2006), requiring an ideal scenario with a considerable magnetic field gradient at the two submillimeter plasma frequency levels to obtain the observed spectral index trend, while keeping the same beam/medium electron density ratio. These qualitative suggestions do not explain other observed features, such as the MW spectral component and the fine time profiles at different wavelength ranges (Kaufmann & Raulin 2006). The microbunching instability by ultrarelativistic electron beams can create bright broadband coherence synchrotron emission observed at MWs and incoherence synchrotron emission in the THz range, similar to what is observed in laboratory accelerators (Kaufmann & Raulin 2006), but requiring very high energy electrons (>10 MeV). Flare-generated electrons gyrating in a magnetic field produce strong GS emission across a broad range of frequencies (e.g., Bastian et al. 1998; Nindos et al. 2008; Zhou et al. 2008). Silva et al. (2007) have demonstrated that a rising optically thick GS spectrum in the THz range requires a large magnetic field (>4500 G) and a high number density of energetic electrons of 1.7×10^{12} $\mathrm{cm^{-3}}$ in a very compact source ~1″ in the uniform magnetic field assumption. In the nonuniform magnetic dipole field assumption, these requirements can be considerably decreased for this flare (Zhou et al. 2010).

In this paper, we investigate another new increasing submillimeter spectral component of an X28 solar flare on 2003 November 4. Our calculations show that both spectral components at submillimeter and MW wavelengths can be explained by the GS emission. The intense increasing submillimeter spectral component during the main peak P1 can be generated, via GS emission, from energetic electrons with harder spectral index (2.3), higher low-energy cutoff of 30 keV, and a number density of 10^{10} $\mathrm{cm^{-3}}$ in a compact source (0.″5 radius) with a strong local magnetic field varying from 780 to 4590 G (with a mean value of 2690 G). On the other hand, the associated traditional MW spectral component is produced by energetic electrons with a 10 keV low-energy cutoff and number density of 1.2×10^{6} $\mathrm{cm^{-3}}$ in an extended source (40″ radius) with

average magnetic field strengths varying from 100 to 576 G (i.e., a mean value of 338 G). For the peak P4 of the submillimeter emission, the required number density is 5.5×10^9 cm^{-3}, i.e., about one-half of the number density of the main peak P1. On the other hand, the number density (6×10^5 cm^{-3}) of the MW source for peak P4 also decreased to half its value compared with that for peak P1. The MW and THz emission sources, inferred from the magnetic dipole field model, are located in the corona from 60,000 to 18,000 km and lower atmosphere levels from 30,000 to ~1000 km above the photosphere, respectively. The THz and MW emissions come from the same flare-accelerated electrons that emit the hard X- and γ-rays, but with a different lower-energy cutoff. We suggest that the new increasing submillimeter component is generated by energetic electrons with higher low-cutoff energy precipitating into the deeper solar atmosphere levels (about 30000–1000 km above the photosphere) and gyrating in very intense magnetic fields. However, the MW spectral component is generated by energetic electrons with lower low-cutoff energy precipitating into the solar corona atmosphere levels and gyrating in mean magnetic fields.

The energy flux of energetic electrons during the flare is estimated from the electron distribution and the low-energy cutoff obtained from the fit to the observed spectrum. It was found that the energy flux in the submillimeter source for the main peak P1 is four orders of magnitude higher than that in the MW source. The energy loss rate of the energetic electrons is also calculated taking a source radius of 0.″5 and 0.″25 for the submillimeter source and 40″ for the MW source, respectively. For the main peak P1 and minor peak P4, the energy loss rate E' reaches 3.0×10^{29} and 4.0×10^{28} erg s^{-1} in the submillimeter source and 4.8×10^{28} and 2.5×10^{28} erg s^{-1} in the MW source, respectively. For the peak P1, the energy loss rate E' in the submillimeter source is about five times higher than that in the MW source due to the strong emission loss in the submillimeter source. The energy E released by the electrons in the MW and submillimeter sources reaches, respectively, 1.9×10^{31} and 1.2×10^{32} erg for about a 400 s time interval, estimated from full width at half-maximum of the burst time profile. The total energy released in the submillimeter and MW sources is 1.4×10^{32} erg during the flare, which is about two orders of magnitude lower than the value of 1.3×10^{34} erg estimated from the hard X-ray emission and two times higher than the value of about 5×10^{31} estimated from *GOES* observations for the EM and temperature.

The GS emission model can easily account for the observed temporal pulsations of the THz component via fluctuations of fast electron injection (Aschwanden et al. 1998). The mean spectrum of the pulse flux in excess of the bulk emission can also be fitted by a GS emission spectrum for a 30 keV low-energy cutoff and electron number density 8.5×10^7 cm^{-3}. The mean energy released by the energetic electrons for a subsecond pulse, i.e., the fragment energy, is estimated to be about 5.2×10^{26} erg.

This paper shows that all the information about the electrons and magnetic fields can be obtained simultaneously from the spectral fit based on the GS computations in the case of a nonuniform magnetic field model, with no further assumptions nor data being necessary. In addition, in the nonuniform magnetic field model, the required local magnetic field strength and number density of electrons in the submillimeter source is much smaller than that in the uniform source case, so that the results obtained in the nonuniform magnetic field model are closer to the real physical parameters of flare loops.

The novel characteristic of this flare at radio wavelengths is its spectral component increasing at >200 GHz frequencies, distinct from the well-known broadband spectral component observed at MWs. Based on our study of the 2003 November 4 flare, we find that the most likely source is the GS radiation from nonthermal electrons, but even this explanation may require adopting high local magnetic fields (~2690 G) and a very small source size (~1″). Fundamental questions remain unanswered: how and where are ultrarelativistic electrons accelerated in a solar flare? Is the submillimeter wave emitting source located in the corona or close to the photosphere and how large is the emitting source? Further progress in understanding the physics of THz emission from flares requires observations with a more complete spectral coverage at the THz range and polarization measurements of higher spatial resolution.

The authors are grateful for the referee's suggestions. This study is supported by the NFSC project Nos. 10833007 and 10703013. We thank Ning Zongjun for helpful discussions and Wang Rongchuan for his help with the calculations.

REFERENCES

Aschwanden, M. J., Kliem, B., Schwarz, U., Kurths, J., Dennis, B. R., & Schwartz, R. A. 1998, ApJ, 505, 941
Bastian, T. S., Benz, A. O., & Gary, D. E. 1998, ARA&A, 36, 131
Bastian, T. S., & Gary, D. E. 1992, Sol. Phys., 139, 357
Batchelor, D. A., Benz, A. O., & Wiehl, H. J. 1984, ApJ, 280, 879
Dulk, G. A. 1985, ARA&A, 23, 169
Dulk, G. A., & Marsh, K. A. 1982, ApJ, 259, 350
Fleishman, G. D., & Kontar, E. P. 2010, ApJ, 709, L127
Gary, D. E. 1985, ApJ, 297, 799
Kane, S. R., McTiernan, J. M., & Hurley, K. 2005, A&A, 433, 1133
Kaufmann, P., & Raulin, J.-P. 2006, Phys. Plasmas, 13, 070701
Kaufmann, P., et al. 2001, ApJ, 548, L95
Kaufmann, P., et al. 2002, ApJ, 574, 1059
Kaufmann, P., et al. 2004, ApJ, 603, L121
Lim, J., White, S. M., Kundu, M. R., & Gary, D. E. 1992, Sol. Phys., 140, 343
Lüthi, T., Magun, A., & Miller, M. 2004, A&A, 415, 1123
Murphy, R. J., Dermer, C. D., & Ramaty, R. 1987, ApJS, 63, 721
Nindos, A., Aurass, H., Klein, K.-L., & Trottet, G. 2008, Sol. Phys., 253, 3
Ohki, K., & Hudson, H. S. 1975, Sol. Phys., 43, 405
Raulin, J. P., Makhmutov, V. S., Kaufmann, P., Pacini, A. A., Lüthi, T., Hudson, H. S., & Gary, D. E. 2004, Sol. Phys., 223, 181
Sakai, J. I., & Nagasugi, Y. 2007, A&A, 470, 1117
Sakai, J. I., Nagasugi, Y., Saito, S., & Kaufmann, P. 2006, A&A, 457, 313
Silva, A. V. R., Share, G. H., Murphy, R. J., Costa, J. E. R., de Castro, C. G. G., Raulin, J.-P., & Kaufmann, P. 2007, Sol. Phys., 245, 311
Stein, W. A., & Ney, E. P. 1963, J. Geophys. Res., 68, 65
Trottet, G. 2006, in Third French-Chinese Meeting on Solar Physics, ed. C. Fang, B. Schmieder, & M. Ding (Nanjing: Nanjing Univ. Press), 82
Trottet, G., Raulin, J.-P., Kaufmann, P., Siarkowski, M., Klein, K.-L., & Gary, D. E. 2002, A&A, 381, 694
Trottet, G., et al. 2004, 35th COSPAR Scientific Assembly, Paris, France, 2234
Zhou, A. H., Huang, G. L., & Li, J. P. 2010, ApJ, 708, 445
Zhou, A.-H., & Karlicky, M. 1994, Sol. Phys., 153, 441
Zhou, A.-H., Li, J.-P., & Wang, X.-D. 2008, Sol. Phys., 247, 63
Zhou, A.-H., Ma, C.-Y., Zhang, J., Wang, X.-D., & Zhang, H.-Q. 1998, Sol. Phys., 177, 427
Zhou, A.-H., Su, Y.-N., & Huang, G.-L. 2004, Chin. Phys. Lett., 21, 2067
Zhou, A.-H., & Wang, X.-D. 2000, Chin. Phys. Lett., 17, 927